Available online at www.sciencedirect.com
ScienceDirect
Trans. Nonferrous Met. Soc. China 31(2021) 744−752
Transactions of Nonferrous Metals Society of China
www.tnmsc.cn

Self-lubricating behavior of $Fe_{22}Co_{26}Cr_{20}Ni_{22}Ta_{10}$ high-entropy alloy matrix composites

Wei-cheng XIAO, Kun LI, Liu-liu HAN, Yong LIU

State Key Laboratory of Powder Metallurgy, Central South University, Changsha 410083, China

Received 8 May 2020; accepted 5 November 2020

Abstract: Eutectic high entropy alloys (EHEAs) have high temperature stability, good mechanical properties, and are promising for tribological applications at high temperatures. To study the high temperature lubrication behavior, $Fe_{22}Co_{26}Cr_{20}Ni_{22}Ta_{10}$−$(BaF_2/CaF_2)_x$ (x=3−20, wt.%) composites were prepared by spark plasma sintering (SPS), with BaF_2/CaF_2 eutectic powder used as solid lubricant. The lubrication behavior and mechanical properties were studied at both room and high temperatures. With the increase of the content of BaF_2/CaF_2 eutectic powder, the friction coefficients and the wear rates of the composites at 600 and 800 °C decrease significantly. The composites with eutectic powder content of 15 and 20 wt.% have the best lubricating performance at 600 °C, with low friction coefficient and wear rates, mainly due to the good mechanical properties of EHEA matrix, the lubrication effect of BaF_2/CaF_2 phase and the oxides formed on the worn surface.

Key words: eutectic high entropy alloy; self-lubricating composite; BaF_2/CaF_2 eutectic powder; tribological properties; microstructure

1 Introduction

Self-lubricating materials are important in industry, such as petrochemical, automotive, mining, aerospace and other fields. However, under severe working condition, the operating temperatures sometimes are so high that conventional lubricating systems cannot serve [1,2]. Therefore, the high temperature behavior of self-lubricating materials is very crucial [3−5].

In 1930s, powder metallurgical metal-based self-lubricating composites were developed [6], generally composed of metallic matrix and ceramic or mineral solid-lubricating phases [7]. The matrix phase can provide sufficient mechanical properties and high temperature oxidation resistance. The most commonly used matrix for high temperature self-lubricating composites are Ni- and Co-based superalloys. The lubricating phases include inorganic fluorides, metal oxides and other ternary compounds. However, the chemical properties between solid lubricants and metals are quite different, and the addition of solid lubricants will reduce the sintering ability of the composites and mechanical properties [8,9]. Therefore, it is important to achieve a balance between the mechanical properties and the tribological properties when designing self-lubricating composites.

High-entropy alloys (HEAs) are becoming more and more important in metallic materials [10−13]. Although HEAs generally contain at least four principal elements, they have a simple structure and excellent properties [14−16]. Recently, LU et al [17] proposed a new kind of HEAs, eutectic high entropy alloys (EHEAs). EHEAs have several features, such as good high-

Corresponding author: Kun LI; Tel: +86-731-88877322; E-mail: kunlee@csu.edu.cn
DOI: 10.1016/S1003-6326(21)65535-8

temperature creep resistance, stable microstructures and high hardness [18]. Therefore, EHEAs are promising for using as high temperature self-lubricating composites. However, there are few studies on EHAs or EHEAs with self-lubrication phases. HAN et al [19] prepared Fe−16.4Mn−4.8Ni−9.9Al−*x*C (wt.%) composites by spark plasma sintering (SPS), and showed a significant improvement in tribological performance due to the self-lubricating effect of graphite. ZHANG et al [20,21] used CoCrFeNi as matrix, and different solid lubricants such as Ag, Cu and fluorides, and showed a better performance of lubrication and higher wear resistance than those of pure HEAs.

In our previous study, FeCoCrNiTa EHEA has excellent mechanical properties and high-temperature stability. It consists of face-centered-cubic (FCC) and Laves phases, and it can be a promising candidate for engineering applications at elevated temperatures [22,23]. In this work, $Fe_{22}Co_{26}Cr_{20}Ni_{22}Ta_{10}$ EHEA matrix composites were prepared by SPS. BaF_2/CaF_2 eutectic was selected to be solid lubricant because its excellent lubrication performance and high temperature stability. The microstructural evolutions and lubrication properties of the EHEA composites were investigated.

2 Experimental

Gas-atomized $Fe_{22}Co_{26}Cr_{20}Ni_{22}Ta_{10}$ powder and BaF_2/CaF_2 eutectic powder were mixed and filled in a graphite die with a diameter of 28 mm. The preparation method of BaF_2/CaF_2 eutectic powder was reported in Refs. [24,25]. The proportions of the raw materials are listed in Table 1. The powder was sintered at 1373 K in the SPS Equipment (HPD25/3), and held for 15 min at 30 MPa, followed by furnace cooling.

Table 1 Compositions of EHEA composites

Sample	Composition/wt.%	
	EHEA	BaF_2/CaF_2
S_1	97	3
S_2	94	6
S_3	91	9
S_4	85	15
S_5	80	20

The X-ray diffractometer (XRD, Rigaku D/MAX−2250, Japan) using a Cu K_α radiation was used to analyze the phase compositions. Scanning electron microscope (SEM, Quanta FEG 250) equipped with an energy dispersive X-ray spectroscopy (EDS) analyzer was used to observe the microstructures of the self-lubricating composites. To further identify the chemical compositions of phases, electron probe micro-analyses (EPMA) was used. The Archimedes method was used to measure the density of the composites. The Vicker's hardness instrument with a load of 0.5 N was used to measure the micro-hardness.

The dry wear tests at room temperature, 600 °C and 800 °C were carried out on a rotational ball-on-disk high temperature tribometer in air. The ball used was Si_3N_4 with a size of 6 mm. The self-lubricating composites were cut in the form of disks with a size of *d*28 mm × 5 mm. The rotation diameter, sliding speed, loads and sliding time of tests were 4 mm, 0.28 m/s, 20 N and 30 min, respectively. Each sample was tested three times, with each time of 30 min. After testing, the worn surfaces were observed by using SEM. A 3D surface profilometer (NT9100, Veeco) was used to measure the worn volume of composites. A micro-beam XRD diffractometer (Rigaku Rapid IIR) was used to analyze the phase compositions of the worn surface.

3 Results

3.1 Material characterizations

Figure 1 shows the typical morphologies of the EHEA powder and the fluorides powder. The EHEA powder is spherical, with a particle size less than 50 μm.

Figure 2 shows the XRD patterns of self-lubricating composites. The FCC phase, Laves phase, fluorides phase (BaF_2 and CaF_2) can be obviously observed. With the increase of the content of BaF_2/CaF_2 eutectic powder, there are stronger peaks corresponding to BaF_2 and CaF_2 phases in the XRD patterns. This result suggests that the BaF_2/CaF_2 eutectic powder does not react heavily with the matrix during SPS.

Figure 3 demonstrates the microstructures of the composites, and Fig. 4 shows the compositional

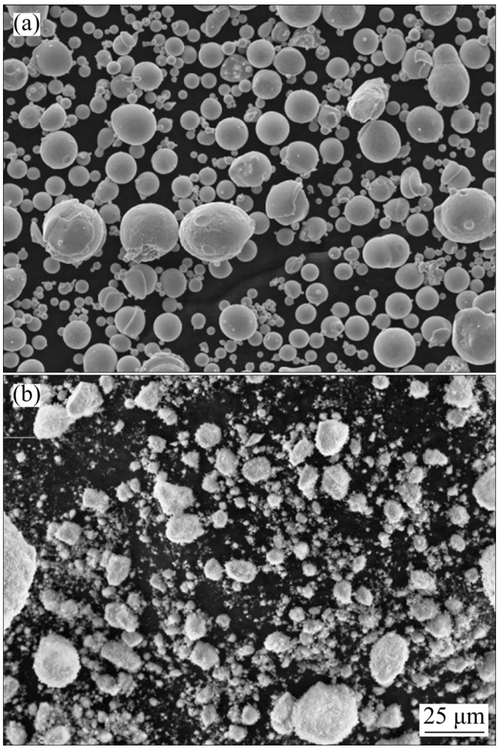

Fig. 1 Morphologies of EHEA powder (a) and BaF_2/CaF_2 eutectic powder (b)

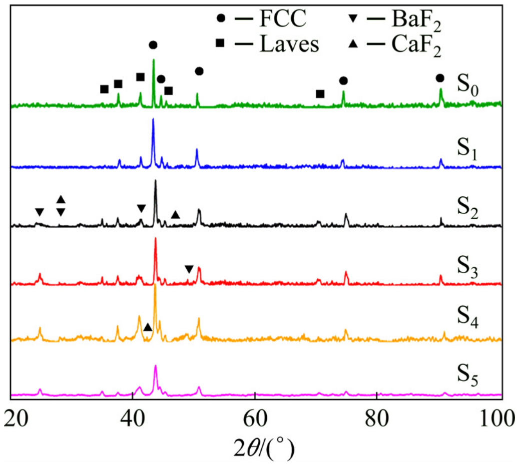

Fig. 2 XRD patterns of different composites

profiles. The grey phase is rich in Co, Cr, Fe and Ni, the white phase rich in Ta, and the dark phase rich in Ba, Ca and F. This indicates that the grey phase is FCC phase, the white phase is Laves phase, and the dark phase is of fluorides. From the results of XRD and microstructure of Sample S_3, the fluorides uniformly distribute and have chemical stability in the matrix.

3.2 Mechanical properties

According to Table 2, the density of the S_1 to S_4 composites is in the range of 9.11−7.31 g/cm^3,

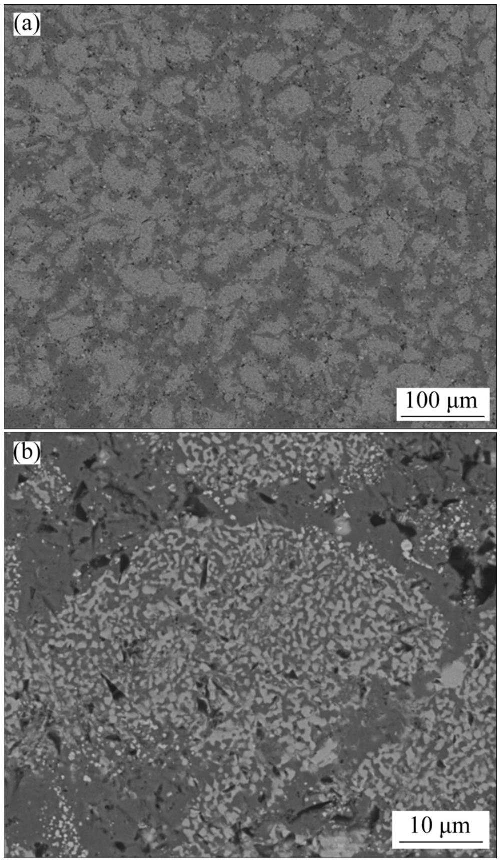

Fig. 3 Microstructures of Sample S_3 sintered at 1100 °C: (a) Low magnification; (b) High magnification

above 99% theoretical value of all composites. When the content of BaF_2/CaF_2 eutectic powder is increased to 20 wt.% (Sample S_5), the relative density decreases.

The hardness of the composites gradually decreases with the increasing content of BaF_2/CaF_2 from 545 HV to 399 HV. The microhardness values of the FCC matrix phase and the Laves phase are higher than those of fluorides phase.

3.3 Friction and wear behavior

The coefficient of frictions (COFs) with the testing time is shown in Fig. 5. Compared to Samples S_1 and S_2, the high-temperature COFs of Samples S_3, S_4 and S_5 decrease obviously. And the COFs of Samples S_4 and S_5 are more stable.

The wear rates and averaged COFs of composites at different temperatures are shown in Fig. 6. The COFs of composites decrease at high temperature, and the COFs of Samples S_3, S_4 and S_5 decrease dramatically. As the content of BaF_2/CaF_2 increases to 9 wt.%, the averaged COF of Sample S_3 decreases to 0.22 at 600 °C, and the wear rate

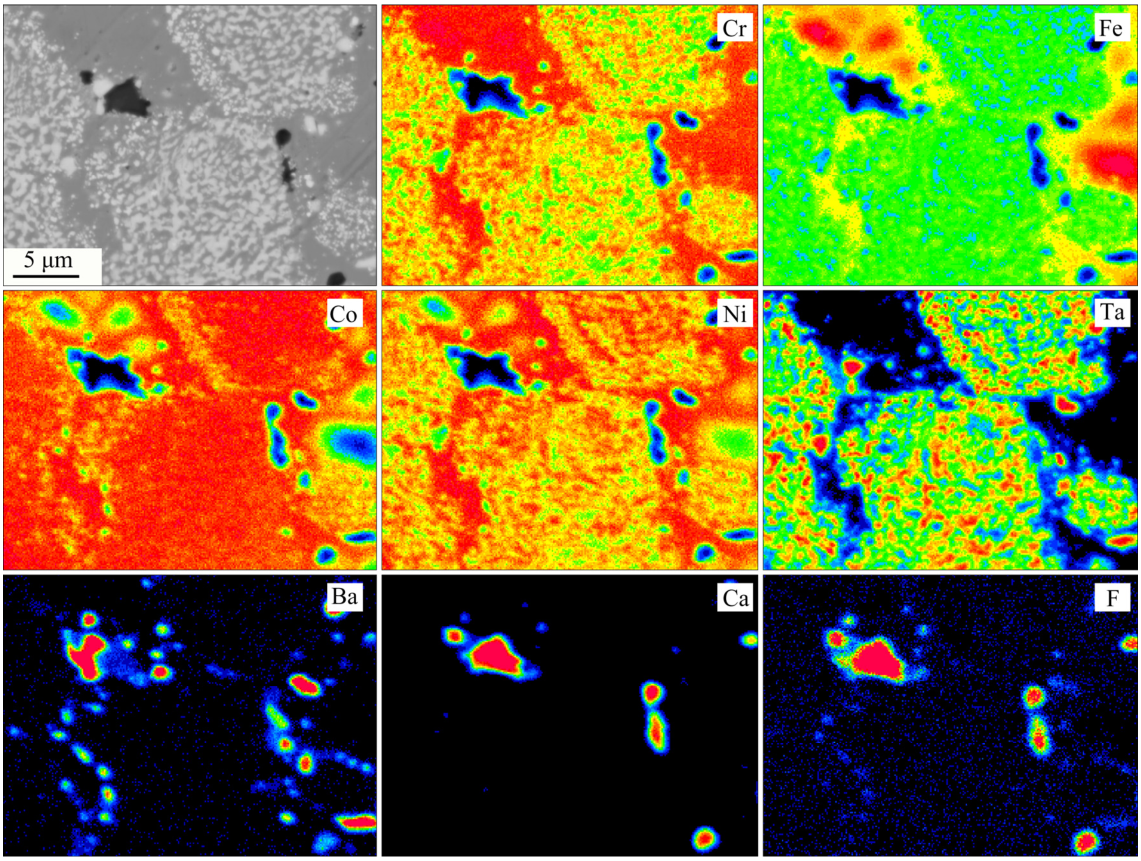

Fig. 4 Microstructure and corresponding elemental mappings of Cr, Fe, Co, Ni, Ta, Ba, Ca and F in Sample S_3

Table 2 Density and hardness of EHEA matrix composites

Sample	Density/ $(g\cdot cm^{-3})$	Relative density/%	Hardness (HV)
S_1	9.11±0.05	99.2±0.1	545±15
S_2	8.79±0.03	99.2±0.1	524±22
S_3	8.51±0.04	99.3±0.2	513±8
S_4	7.87±0.03	99.1±0.1	467±6
S_5	7.31±0.07	97.2±0.3	399±25

maintains to be 5.9×10^{-5} $mm^3/(N\cdot m)$. Further increasing the content of BaF_2/CaF_2, the COF becomes more stable and maintains around 0.22. The wear rates of the composites are in the magnitude of 10^{-5} $mm^3/(N\cdot m)$. With temperature increasing, the wear rate decreases.

In order to investigate the wear mechanism, the worn surface of the composites was analyzed, and the results are shown in Fig. 7 and Table 3. Some plowing grooves can be observed on the worn surfaces, suggesting that slight abrasive wear happens. Adhesive wear also occurs during the wear process, evidenced by the formation of patches and the transfer of materials. According to the change of O content in the EDS result, severe oxidation occurs at high temperatures.

The COF of Sample S_2 is about 0.35 at 600 °C, which is the same as that of Sample S_1. According to Fig. 7, the wear mechanisms of S_2 are adhesive wear, abrasive wear and oxidation wear. With the increase of BaF_2/CaF_2 content, the worn surface of S_2 forms a discontinuous and broken glassy layer, which may lost the self-lubricating ability.

The worn surfaces of Sample S_3 tested at RT have similar morphology with Samples S_1 and S_2, showing adhesive wear and slightly abrasive wear. With temperatures increasing to 600 and 800 °C, the worn surfaces of the composites become smooth, and the continuous glassy layers form on the worn surfaces. According to the EDS results, the Ba, Ca and F contents of the glassy layer (Region 8) are higher than those of the rough surface (Region 9). This result is mainly due to the fact that the glassy layer is rich in fluorides.

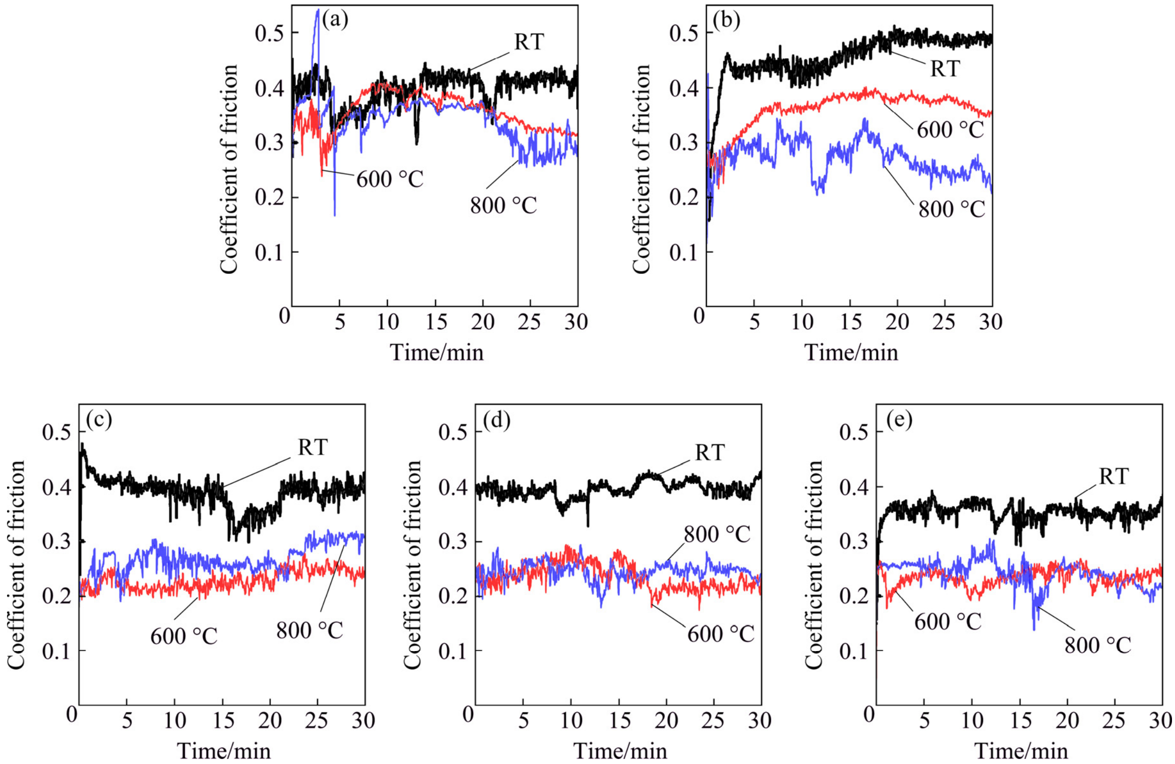

Fig. 5 COFs with sliding time of different composites: (a) Sample S_1; (b) Sample S_2; (c) Sample S_3; (d) Sample S_4; (e) Sample S_5

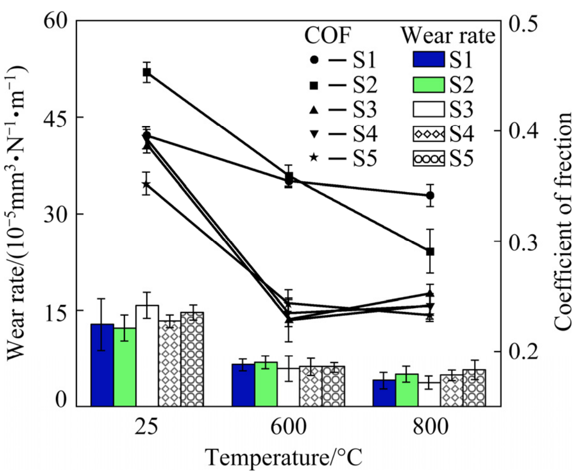

Fig. 6 Wear rates and averaged COFs of different composites with temperature

With further increasing of BaF_2/CaF_2 content, the whole worn surface of Samples S_4 and S_5 is similar to those of Sample S_3 after testing at RT, 600 °C and 800 °C. The glassy layers form on the worn surface at high temperatures, which are rich in fluorides. In summary, the major wear behavior of Samples S_4 and S_5 is almost the same with that of Sample S_3.

To further study the lubricating behavior of Sample S_3 at high temperatures, the cross-sectional microstructure and EDS results of the worn surface at 600 °C are shown in Fig. 8 and Table 4. The Ba, Ca and F contents of the glassy layer (Region A) are higher than those of the composite (Region B). The thickness of the continuous glassy layer is about 7 μm, which is bonded with the composite closely.

Figure 9 shows the micro-beam XRD patterns of Sample S_3 after testing at RT, 600 °C and 800 °C. At RT, FCC phase, Laves phase, BaF_2 and CaF_2 are observed, and no peaks of oxides appear on the worn surface. At 600 and 800 °C, the glassy layer mainly consists of different metal oxides (Cr_2O_3, Fe_2O_3 and other oxides) and BaF_2/CaF_2 eutectic phase.

4 Discussion

4.1 Microstructures

In this work, the EHEA matrix composites were prepared by SPS with microstructures consisting of FCC phase, Laves phase, BaF_2 and CaF_2. Fluoride phases distribute homogeneously in

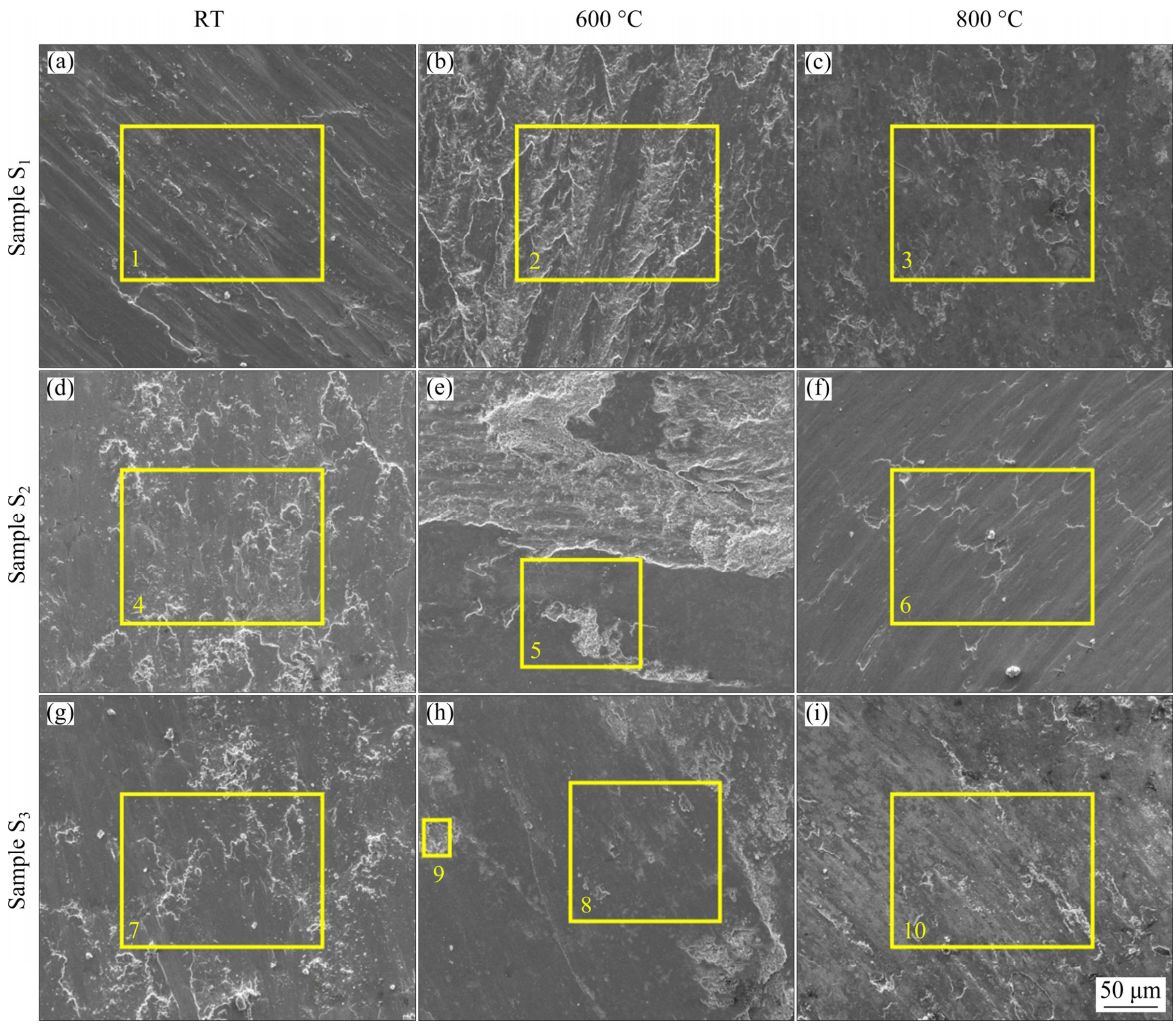

Fig. 7 Morphologies of worn surface and marked areas for EDS

Table 3 Compositions of regions on worn surfaces marked in Fig. 7

Region No.	Composition/at.%									
	Fe	Co	Cr	Ni	Ta	Ba	Ca	F	O	Si
1	19.5±1.3	20.7±0.3	14.7±0.3	18.8±0.5	8.4±0.4	0.6±0.1	0.9±0.1	2.4±0.7	11.2±1.2	2.7±0.1
2	14.4±0.5	14.1±0.4	9.3±0,9	9.5±0.1	3.0±1.1	0.5±0.1	0.7±0.5	2.3±1.0	43.9±2.1	2.3±0.2
3	10.9±0.4	11.9±1.1	9.5±1.1	8.6±0.1	2.8±0.2	0.6±0.1	0.6±0.1	2.4±0.4	50.6±1.9	2.1±0.1
4	18.2±1.1	18.8±1.0	14.3±0.9	17.4±0.5	6.9±0.4	1.3±0.2	1.8±0.7	5.5±0.4	13.5±1.1	2.5±0.3
5	11.6±0.4	10.6±0.4	7.9±0.9	8.1±0.1	3.1±0.2	1.6±0.2	1.7±0.2	8.7±0.1	43.9±1.2	2.8±0.4
6	9.4±1.4	9.7±0.2	6.7±0.8	9.9±0.2	2.5±0.1	1.5±0.1	1.4±0.7	6.0±0.6	50.8±1.1	2.1±0.1
7	15.9±1.3	19.0±0.5	17.4±0.1	18.2±0.9	4.7±0.1	1.3±0.4	2.2±0.7	8.9±0.3	9.5±1.5	2.9±0.2
8	8.8±0.2	9.5±0.6	9.7±0.3	9.8±0.2	1.9±0.4	2.2±0.5	3.8±0.9.	9.7±0.2	41.9±1.6	2.7±0.1
9	9.1±0.5	9.7±0.1	10.0±0.1	9.6±02.	4.9±0.2	1.9±0.2	1.9±0.3	4.3±0.1	46.3±1.1	2.3±0.9
10	7.2±0.4	7.2±0.3	7.4±0.2	7.3±0.1	2.3±0.1	2.3±0.2	3.8±0.2	10.5±0.1	49.9±1.2	2.1±0.7

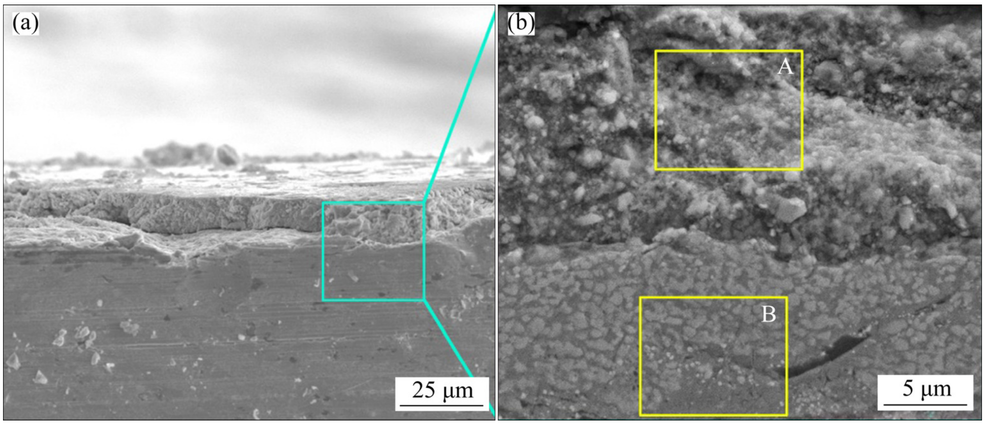

Fig. 8 Microstructures of cross-sections of worn Sample S_3 after testing at 600 °C

Table 4 Compositions of regions on worn surface marked in Fig. 8

Region	Composition/at.%								
	Fe	Co	Cr	Ni	Ta	Ba	Ca	F	O
A	12.7±0.5	8.2±0.3	8.1±0.8	8.4±0.4	2.2±0.4	2.4±0.1	3.1±0.1	9.2±0.2	45.7±1.1
B	20.7±0.1	20.2±0.7	17.8±0.2	17.9±0.3	8.5±0.3	0.9±0.2	1.5±0.2	8.1±0.2	4.4±0.5

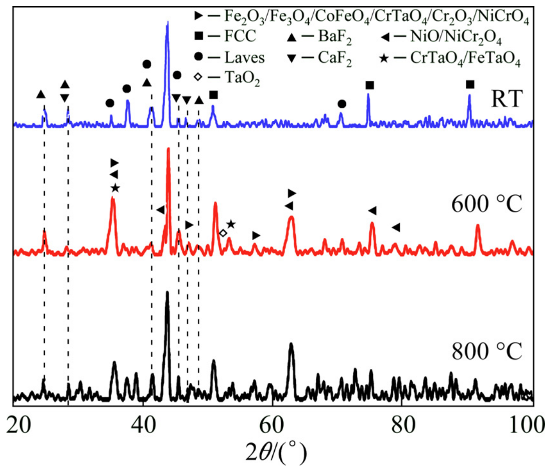

Fig. 9 Micro-beam XRD patterns of Sample S_3 after testing at different temperatures

the EHEA matrix, and have good chemical stability. This distribution makes the microstructure uniform, and also makes it easier to form a complete and continuous lubrication layer during the wear process.

The melting point of BaF_2/CaF_2 eutectic phase is lower than the sintering temperature, so the fluoride phases mostly distribute in the pores of the matrix. The liquid phase sintering can further improve the density of the composites [26], but excessive liquid phase during the sintering process will have an adverse impact on the mechanical properties of the composites.

4.2 Wear behavior

The smooth and continuous glassy layer formed on the worn surface is the key for decreasing the friction coefficients at high temperatures. When the content of BaF_2/CaF_2 is higher than 9 wt.%, the glassy layers forming on the worn surface can prevent the direct contact between composite disk and SiN_4 ball, which keeps the COF stable and the wear rates low.

The BaF_2/CaF_2 phase is stable at high temperatures, and it has good lubricating properties because of its lower melting point and shear stress. During the sliding test at high temperatures, the BaF_2/CaF_2 eutectic powder can coat on the worn surface easily. Therefore, sufficient and homogeneously distributed BaF_2/CaF_2 eutectic phase in the matrix is the very important for the self-lubricating effect. In addition, the oxides may soften at high temperatures and easily form a continuous layer with the BaF_2/CaF_2 eutectic phase. Therefore, the metal oxides can also improve lubricating properties at high temperatures.

For metallic solid self-lubricating materials, the lubricating phase can decrease the mechanical properties. It is important to find a balance between lubricating properties and mechanical properties. When the composite has 9−15 wt.% lubricants (Samples S_3 and S_4), it has the best combination of lubricating and mechanical properties (Table 5).

Table 5 Wear properties of Samples S_3 and S_4 and other powder metallurgy (PM) HEA self-lubricating materials

Sample	Hardness (HV)	COF (600°C)	Wear rate (600 °C)/ $(mm^3 \cdot N^{-1} \cdot m^{-1})$	Load/N	Counterpart
S_3	513	0.22	5.9×10^{-5}	20	SiN_4
S_4	467	0.23	6.2×10^{-5}	20	SiN_4
$CoCrFeNiS_{0.5}$ [20]	259	0.3	10×10^{-5}	5	SiN_4
CoCrFeNi−Ag/BaF_2/CaF_2 [21]	151	0.26	15×10^{-5}	5	GCr_{15}
CoCrFeNi−C/MoS_2 [26]	271	0.3	8×10^{-5}	5	SiN_4
Fe−Mn−Ni−Al−C [19]	566	0.42	1×10^{-5}	20	SiN_4

Compared with other self-lubricating materials of almost the same type of compositions (Table 5), the composites in this work have lower COFs and wear rates at 600 °C. In summary, the EHEA composites may have potential applications in high temperature service.

5 Conclusions

(1) The phase compositions of $Fe_{22}Co_{26}Cr_{20}$-$Ni_{22}Ta_{10}$−BaF_2/CaF_2 composites are of FCC, Laves phase, BaF_2, and CaF_2. The BaF_2 and CaF_2 show high chemical stability with the EHEA.

(2) The hardness of $Fe_{22}Co_{26}Cr_{20}Ni_{22}Ta_{10}$−$BaF_2$/$CaF_2$ composite gradually decreases with the increase of BaF_2/CaF_2 eutectic powder content from HV 545 to HV 399.

(3) The EHEA composites show good lubricating performance at high temperatures. When the content of BaF_2/CaF_2 eutectic powder is 9−15 wt.%, both the COF and the wear rate at high temperatures are lower than other FeCoCrNi-based composites. The good lubricating performance is due to the effect of BaF_2/CaF_2 eutectic phase, the formation of complex oxides, and high hardness of the matrix.

Acknowledgments

The authors acknowledge the financial support from the National Natural Science Foundation of China (51671217).

References

[1] HAYAJNEH M T, HASSAN A M, MAYYAS A T. Artificial neural network modeling of the drilling process of self-lubricated aluminum/alumina/graphite hybrid composites synthesized by powder metallurgy technique [J]. Journal of Alloys and Compounds, 2009, 478: 559−565.

[2] NIU Mu-ye, BI Qin-ling, ZHU Sheng-yu, YANG Jun, LIU Wei-min. Microstructure, phase transition and tribological performances of Ni_3Si-based self-lubricating composite coatings [J]. Journal of Alloys and Compounds, 2013, 555: 367−374.

[3] LI Zhen-wei, DI Shi-chun. Preparation and properties of micro-arc oxidation self-lubricating composite coatings containing paraffin [J]. Journal of Alloys and Compounds, 2017, 719: 1−14.

[4] CUI Gong-jun, LU Lei, WU Juan, LIU Yan-ping, GAO Gui-jun. Microstructure and tribological properties of Fe−Cr matrix self-lubricating composites against Si_3N_4 at high temperature [J]. Journal of Alloys and Compounds, 2014, 611: 235−242.

[5] NARAYANASAMY P, SELVAKUMAR N. Tensile, compressive and wear behaviour of self-lubricating sintered magnesium based composites [J]. Transactions of Nonferrous Metals Society of China, 2017, 27(2): 312−323.

[6] WANG Chang-chuan, WANG Ri-chu, PENG Chao-qun, FENG Yan, WEI Xiao-feng. Research progress of metallic solid self-lubricating composites [J]. The Chinese Journal of Nonferrous Metals, 2012, 22(7): 1945−1955. (in Chinese)

[7] WU Yun-xin, WANG Fu-xing, CHENG Yin-qian, CHEN Nan-ping. A study of the optimization mechanism of solid lubricant concentration in $NiMoS_2$ self-lubricating composite [J]. Wear, 1997, 205(1−2): 64−70.

[8] SHI Xiao-liang, YAO Jie, XU Zeng-shi, ZHAI Wen-zheng, SONG Si-yuan, WANG Mang, ZHANG Qiao-xin. Tribological performance of TiAl matrix self-lubricating composites containing Ag, Ti_3SiC_2 and BaF_2/CaF_2 tested from room temperature to 600 °C [J]. Materials & Design, 2014, 53: 620−633.

[9] SHI Xiao-liang, WANG Mang, ZHAI Wen-zheng, XU Zeng-shi, ZHANG Qiao-xin, CHEN Ying. Influence of Ti_3SiC_2 content on tribological properties of NiAl matrix self-lubricating composites [J]. Materials & Design, 2013, 45: 179−189.

[10] ANTONAGLIA J, XIE X, TANG Z, TSAI C, QIAO J, ZHANG Y, LAKTIONOVA M O, TABACHNIKOVA E D, YEH J W, SENKOV O N, GAO M C, UHL J T, LIAW P K, DAHMEN K A. Temperature effects on deformation and serration behavior of high-entropy alloys (HEAs) [J]. JOM, 2014, 66(10): 2002−2008.

[11] MIRACLE D B, SENKOV O N. A critical review of high entropy alloys and related concepts [J]. Acta Materialia, 2017,

122: 448−511.

[12] CANTOR B, CHANG I T H, KNIGHT P, VINENT A J B. Microstructural development in equiatomic multicomponent alloys [J]. Materials Science and Engineering A, 2004, 375: 213−218.

[13] YEH J W. Alloy design strategies and future trends in high-entropy alloys [J]. JOM, 2013, 65(12): 1759−1771.

[14] HE Feng, WANG Zhi-jun, WU Qing-feng, LI Jun-jie, WANG Jin-cheng, LIU C T. Phase separation of metastable CoCrFeNi high entropy alloy at intermediate temperatures [J]. Scripta Materialia, 2017, 126: 15−19.

[15] TANG Zhi, YUAN Tao, TSAI C W, YEH J W, LUNDIN C D, LIAW P K. Fatigue behavior of a wrought $Al_{0.5}CoCrCuFeNi$ two-phase high-entropy alloy [J]. Acta Materialia, 2015, 99: 247−258.

[16] POLETTI M G, FIORE G, GILI F, MANGHERINI D, BATTEZZATI L. Development of a new high entropy alloy for wear resistance: $FeCoCrNiW_{0.3}$ and $FeCoCrNiW_{0.3}$+ 5 at.% of C [J]. Materials & Design, 2017, 115: 247−254.

[17] LU Yi-ping, JIANG Hui, GUO Sheng, WANG Tong-min, CAO Zhi-qiang, LI Ting-ju. A new strategy to design eutectic high-entropy alloys using mixing enthalpy [J]. Intermetallics, 2017, 91: 124−128.

[18] LU Yi-ping, DONG Yong, JIANG Hui, WANG Zhi-jun, CAO Zhi-qiang, GUO Sheng, WANG Tong-min, LI Ting-ju, LIAW P K. Promising properties and future trend of eutectic high entropy alloys [J]. Scripta Materialia, 2020, 187: 202−209.

[19] HAN Liu-liu, LI Kun, QIAN Cheng, QIU Jing-wen, ZHOU Cheng-shang, LIU Yong. Wear behavior of light-weight and high strength Fe−Mn−Ni−Al matrix self-lubricating steels [J]. Journal of Materials Science & Technology, 2019, 35(4): 623−630.

[20] ZHANG Ai-jun, HAN Jie-sheng, SU Bo, MENG Jun-hu. A promising new high temperature self-lubricating material: $CoCrFeNiS_{0.5}$ high entropy alloy [J]. Materials Science and Engineering A, 2018, 731: 36−43.

[21] ZHANG Ai-jun, HAN Jie-sheng, SU Bo, MENG Jun-hu. A novel CoCrFeNi high entropy alloy matrix self-lubricating composite [J]. Journal of Alloys and Compounds, 2017, 725: 700−710.

[22] HAN Liu-liu, XU Xian-dong, WANG Li, PYCZAK F, ZHOU Rui, LIU Yong. A eutectic high-entropy alloy with good high-temperature strength-plasticity balance [J]. Materials Research Letters, 2019, 7: 460−466.

[23] HAN Liu-liu, XU Xian-dong, LI Zhi-ming, LIU Bin, LIU Yong. A novel equiaxed eutectic high-entropy alloy with excellent mechanical properties at elevated temperatures [J]. Materials Research Letters, 2020, 8(10): 373−382.

[24] DING C H, YANG Z M, ZHANG H, GUO Y, ZHOU J C. Microstructure and tensile strength of PM304 composite [J]. Composites Part A: Applied Science and Manufacturing, 2007, 38(2): 348−352.

[25] KONG Ling-qian, BI Qin-ling, ZHU Sheng-yu, YANG Jun, LIU Wei-min. Tribological properties of ZrO_2 (Y_2O_3)−Mo−BaF_2/CaF_2 composites at high temperatures [J]. Tribology International, 2012, 45(1): 43−49.

[26] ZHANG Ai-jun, HAN Jie-sheng, SU Bo, LI Peng-de, MENG Jun-hu. Microstructure, mechanical properties and tribological performance of CoCrFeNi high entropy alloy matrix self-lubricating composite [J]. Materials & Design, 2016, 114: 253−263.

$Fe_{22}Co_{26}Cr_{20}Ni_{22}Ta_{10}$高熵合金基复合材料的自润滑性能

肖维城，李 昆，韩六六，刘 咏

中南大学 粉末冶金国家重点实验室，长沙 410083

摘　要：共晶高熵合金(EHEAs)具有高温稳定性和良好的力学性能，并有望在高温下应用于摩擦领域。为了研究其高温润滑性能，采用 BaF_2/CaF_2 共晶粉末作为润滑相，通过放电等离子烧结制备 $Fe_{22}Co_{26}Cr_{20}Ni_{22}Ta_{10}$−($BaF_2/CaF_2$)$_x$ (x=3%~20%，质量分数)复合材料，在室温和高温下测试摩擦性能和力学性能。结果表明，随着 BaF_2/CaF_2 共晶粉末的增加，复合材料在 600 和 800 °C 时的摩擦因数和磨损率明显降低。其中，共晶粉末含量为 15%和 20%的复合材料在 600 °C 时具有最佳的润滑性能。复合材料的低摩擦因数和低磨损率主要归功于共晶高熵合金基体良好的力学性能、BaF_2/CaF_2 相的润滑作用以及在磨损表面上形成的连续氧化物。

关键词：共晶高熵合金；自润滑复合材料；BaF_2/CaF_2 共晶粉末；摩擦磨损性能；显微组织

(Edited by Bing YANG)